Published in final edited form as:
Arterioscler Thromb Vasc Biol. 2010 March ; 30(3): 403–410. doi:10.1161/ATVBAHA.109.198556.

Magnetic resonance molecular imaging of thrombosis in an arachidonic acid mouse model using an activated platelet targeted probe

Ahmed Klink[1,2], **Eric Lancelot**[3], **Sébastien Ballet**[3], **Esad Vucic**[1], **Jean-Etienne Fabre**[4], **Walter Gonzalez**[3], **Christelle Medina**[3], **Claire Corot**[3], **Willem J. M. Mulder**[1], **Ziad Mallat**[2,*], and **Zahi A. Fayad**[1,5,*]

[1]Translational and Molecular Imaging Institute, Imaging Sciences Laboratories, Department of Radiology, Zena and Michael A. Wiener Cardiovascular Institute; Mount Sinai School of Medicine, New York, NY 10029, USA

[2]Paris Cardiovascular Research Center, INSERM Assistance Publique-Hopitaux de Paris, Hopital Europeen Georges Pompidou, Paris, France

[3]Guerbet, BP57400, F95943, Roissy Charles-de-Gaulle, France.

[4]Institut de Génétique et de Biologie Moléculaire et Cellulaire, Institut National de la Santé et de la Recherche Médicale U964, Centre National de la Recherche Scientifique UMR7104, Université de Strasbourg, 67400 Illkirch, France.

[5]The Zena and Michael A. Wiener Cardiovascular Institute and Marie-Josee and Henry R. Kravis Center for Cardiovascular Health, Mount Sinai School of Medicine, New York, New York, USA.

Abstract

Objective—The non-invasive *in vivo* visualization of activated platelets using a target-specific MRI contrast agent to identify thrombi, hallmarks of vulnerable/high-risk atherosclerotic plaques.

Methods—Inflammatory thrombi were induced in mice via topical application of arachidonic acid on the carotid. Thrombus formation was imaged with intravital fluorescence microscopy and molecular MRI. To accomplish the latter, a paramagnetic contrast agent (P975) that targets the glycoprotein $\alpha_{IIb}\beta_3$ expressed on activated platelets was investigated. The specificity of P975 for activated platelets was studied in vitro. In vivo, high spatial-resolution MRI was performed at baseline and longitudinally over 2 hours after injecting P975 or a non-specific agent. The contralateral carotid, a sham surgery group and a competitive inhibition experiment served as controls.

Results—P975 showed a good affinity for activated platelets with an IC50 value of 2.6 μM. In thrombosed animals, P975 produced an immediate and sustained increase in MRI signal whereas none of the control groups revealed any significant increase in MRI signal 2 hours post-injection. Importantly, the competitive inhibition experiment with a $\alpha_{IIb}\beta_3$ antagonist suppressed the MRI signal enhancement, which is indicative for the specificity of P975 for the activated platelets.

Corresponding Authors: Zahi A. Fayad, Mount Sinai School of Medicine, Translational and Molecular Imaging Institute, Atran BM-24, Box 1234, One Gustave L. Levy Place, New York, NY 10029, USA, Tel: 212-241-6858, Fax: 212-534-2683, zahi.fayad@mssm.edu, Ziad Mallat Paris Cardiovascular Research Center, INSERM Assistance Publique-Hopitaux de Paris, Hoptial, Europeen Georges Pompidou, Paris, France, ziad.mallat@inserm.fr.

Conclusion—P975 allowed *in vivo* target-specific noninvasive MR imaging of activated platelets.

Introduction

Acute thrombus formation is an outcome of atherosclerosis and may trigger the onset of serious clinical events such as myocardial infarction or stroke 1. The rupture or erosion of atherosclerotic plaques exposes the pro-thrombotic core to the blood and is regarded as the pivotal event for thrombus formation 2. Activated platelets play a critical role in thrombogenesis through both platelet aggregation and activation of the coagulation cascade [3–4]. Consequently, platelets have been a target for aggressive treatments in patients suffering from acute coronary syndrome (ACS) and stroke. A specific signature of platelet activation is the externalization of integrins $\alpha_{IIb}\beta_3$ that play a pivotal role in platelet aggregation and thrombogenesis. Indeed, $\alpha_{IIb}\beta_3$ inhibitors are recommended in patients with unstable angina [5]. Hence, $\alpha_{IIb}\beta_3$ might be a good biomarker of nascent thrombosis. Using $\alpha_{IIb}\beta_3$ to image adherent or activated platelets therefore represents a unique opportunity to identify atherothrombosis and vulnerable plaques before they induce dramatic clinical events [3–4].

Currently, most of the imaging techniques for thrombus detection are invasive or are characterized by a relatively poor spatial resolution. However, major advances in medical imaging techniques in general and in non-invasive magnetic resonance techniques in particular, have been achieved in recent years, and allow the visualization of both the vessel wall and atherosclerotic plaques [6–11]. Indeed, our group and others have shown that the visualization of atherothrombotic plaques as well as the identification of vulnerable lesions was achievable through non contrast-enhanced magnetic resonance imaging (MRI) [12]. Nevertheless, complete characterization of plaque components and particularly the accurate identification of thrombi *in vivo* remains a major challenge. Recently, encouraging studies have been published using MR molecular imaging with gadolinium (Gd) contrast agents targeting fibrin to allow thrombi detection 13–14. These studies hold special promises for imaging large occlusive thrombi displaying a high fibrin buildup. Moreover, Von zur Muhlen et al. reported the use of iron oxide microparticles (MPIOs) attached to a single chain antibody targeting activated platelets to image thrombi induced in mice carotid arteries via MRI. The authors showed that contrast agent targeted to activated platelets allowed the sensitive and rapid detection of smaller mural thrombi 15. Molecular imaging of platelets has been demonstrated in patients using nuclear imaging approaches such as single positron emission computed tomography (SPECT) [16–18]. In fact, Acu-tect, a technetium99m label, is FDA approved for this purpose 19. However, MRI will offer superior spatial resolutions and concomitant anatomical information compared to SPECT and nuclear imaging techniques in general.

As of yet, most of the studies about experimental thrombosis have used a ferric chloride model of thrombogenesis [20]. This model does not involve the physiological mechanisms of thrombi formation but rather creates a severe endothelial injury that leads to thrombosis. Recently, an alternative model of thrombosis, in which arachidonic acid (AA) is topically applied to mice carotid arteries, was introduced [21]. One of the major advantages of this model is that it more closely mimics inflammatory thrombogenesis through platelets activation and activation of the coagulation cascade.

In the current study, after emphasizing the critical role of platelets in AA induced thrombi by using intravital microscopy, we used an activated platelet targeted MRI contrast agent to non-invasively monitor the formation of platelet-rich-thrombi in the aforementioned model of thrombosis. This contrast agent (P975, Guerbet, France) is composed of a peptide targeting $\alpha_{IIb}\beta_3$ (P977) conjugated to a Gadolinium chelate (Gd-DOTA). The specificity of P975 to activated human platelets is shown here both *in vitro* and *in vivo*.

Methods

Contrast agent

P975 (Guerbet, France) is a Gd-based contrast agent obtained by coupling a peptide (P977) via a small linker to the Gd chelate 1,4,7,10-tetraazacyclododecane-N,N',N'',N'''-tetraacetic acid (DOTA) at a 1:1 molar ratio. P977 is a cyclic peptide (cyclo(Cys-Arg-Gly-Asp-Cys)) of 878 Da known to bind to the integrin alpha-V-beta-3 expressed on tumor cells [22]. This conformation was also reported to provide a good affinity for $\alpha_{IIb}\beta_3$ [23] and was therefore selected for the design of P975. The targeted contrast agent (P975) has a molecular weight of 1344 Da which is approximately 2.5 times greater than Gd-DOTA.

Measurement of P975 and P977 binding to TRAP-stimulated platelets

The binding of P975 and P977 to the $\alpha_{IIb}\beta_3$ integrin was evaluated by inhibition measurements of specific FITC-Fg binding to TRAP-stimulated platelets using flow cytometry. Fifteen microliters of resting platelets, corresponding to $6–7.5\times10^6$ platelets per vial (calculated by counting), were activated by 100 μM TRAP-6 (Thrombin Receptor Activating Peptide, Bachem) and co-incubated with both increasing concentrations of test compounds P975 and P977 and 200 nM of FITC-Fg [24] for 5 minutes at 37°C. All the reagents were dissolved in Tyrode solution and the binding protocol was performed in 100μl reaction volume. The FITC-Fg binding was then measured by flow cytometry (FC500, Beckman Coulter) specifically gated on the population of platelets (without leukocytes) after excitation with a laser at 488 nm and emission at 525 nm. The specific binding of FITC-Fg to $\alpha_{IIb}\beta_3$ expressed by stimulated platelets was calculated by subtracting the mean of fluorescent signal emitted by non-stimulated platelets from the one of TRAP-stimulated platelets. Tirofiban (Aggrastat®, Merck, Sharp and Dohme, Netherlands) was used as positive control for $\alpha_{IIb}\beta_3$ binding inhibition. For each compound (P975, P977), the inhibition constant Ki was calculated from the Cheng-Prusoff equation:

$$Ki=IC_{50}/[1+(L/Kd)]$$

where IC_{50} represents the concentration yielding 50% inhibition of specific FITC-Fg binding to platelets, L is the FITC-Fg concentration (200 nM), and Kd is the dissociation constant (466 nM in our conditions, data not shown). IC_{50} values were calculated by plotting a graph of fluorescence intensity as a function of the concentration of the inhibitor, and by estimating the concentration that corresponded to a 50% reduction of the maximum of specific fluorescence. The Ki and IC_{50} values were calculated using Graph Pad PRISM® software v4.0.

Imaging of thrombus formation with fluorescent intravital microscopy

Briefly, mouse blood was collected in acid citrate dextrose and centrifuged at 100 g to separate platelets. Platelets were incubated with 300ng/ml calcein AM (Invitrogen, USA) in Tyrode's buffer for 15 minutes in the dark. Washed labeled platelets were injected in the jugular vein of the receiving mice and AA thrombosis was induced in one of the carotids (supplemental methods). The animal was placed under a fluorescent macroscope (MacroFluo; Leica) for video-recording thrombosis at 480 nm.

MRI detection of the arachidonic acid–induced thrombosis

Ten to eleven week old male C57BL/6 mice (*n*=17, Jackson Laboratories, USA) were used in total. Care of use of laboratory animals followed the national guidelines and were approved by The Mount Sinai School of Medicine Animal Committee (IACUC). Immediately after AA thrombus induction (supplemental methods), a venous catheter connected with a 1 ml syringe containing a 100 μmol Gd/kg dose of the contrast agent P975 was placed into the tail vein. The

animals (*n*=5) were placed at the center of a whole-body coil (35 mm inner diameter) under continuous isoflurane anesthesia and positioned in a 9.4 T MRI system (Bruker BioSpec, Bruker, Germany). The animals were connected to a respiratory-rate monitor and the flow of anesthetic gas was constantly regulated to maintain a breathing rate of 60±20 breaths per minute. The imaging protocol consisted of a pilot scan with 3 orthogonal slices followed by a spin echo T1-weighted sequence with an in-plane spatial resolution of 117 μm (slice thickness of 1 mm, field of view of 300 mm, matrix size of 256×256), a repetition time (TR) of 800 ms, an echo time (TE) of 10.2 ms and 4 averages, resulting in an imaging time of 13.26 minutes. The area covered the common carotid artery, the carotid bifurcation and the distal carotid artery. Contiguous cross sectional images were obtained perpendicular to the long axis of the neck. The animals were scanned at baseline – 20 minutes after thrombus induction - and longitudinally over a 2-hour period after a bolus injection of 150 μl of the contrast agent to follow the time course of enhancement. In each animal, the contralateral carotid was used as a negative control.

A second group of mice (n=5) was used to compare P975 to the conventional Gd chelate (Gd-DOTA, 100 μmol Gd/kg, IV). In addition, a third sham surgery group (*n*=2), where the diameter of the carotid was reduced upstream and the AA application was substituted by an application of ethanol (EtOH), was studied.

To demonstrate the *in vivo* specificity of P975 to the integrin $\alpha_{IIb}\beta_3$ expressed on activated platelets, a competitive inhibition experiment on a fourth group of mice was performed (*n*=5). After thrombus induction, a baseline MRI scan was performed. Subsequently, Eptifibatide **(Integrilin^{R})**, a clinically used $\alpha_{IIb}\beta_3$ antagonist (Schering-Plough, Essex, USA), was injected at 10 times the normal murine dose of 1.8 μg/g [25] in order to saturate the integrins prior to P975 administration. Thereafter, P975 was injected and the post-scan procedure was performed according to the protocol described above.

Quantification of MRI signal-enhancement

Image analysis was performed using OsiriX DICOM reader v3.0 (Geneva, Switzerland). At the site of thrombogenesis, the inner vessel boundary was traced to determine the average signal intensity of the lumen in both the thrombosed and the contralateral carotid (SIcarotid). Additional ROIs were placed in the paravertebral muscles and in a motion free region outside the animal to determine the signal intensity of the reference tissue (SImuscle) and the standard deviation of the noise signal (SDnoise), respectively. Individual contrast-to-noise ratios (CNR) were calculated from three contiguous MR images at each imaging time point [CNR= (SIcarotid-SImuscle)/SDnoise]. Their average resulted in a mean CNR value (mCNR). The differences between the mean CNR due to the contrast agent injection (P975 or Gd-DOTA) were determined and plotted over time [ΔCNR=mCNR(imaging timepoint)-mCNR(baseline)]. The evolution of ΔCNR values was compared between all groups. In addition, the ΔCNR values at 2 hours post-injection were plotted and statistical analyses were performed between each group to evaluate late enhancement. A 1-way ANOVA test was performed using Graph Pad PRISM® software v4.0.in order to compare the groups. A p value inferior to 0.05 was considered to indicate a significant difference between the groups.

Histopathology

Histological evaluation of the thrombus and correlation of thrombus localization with MRI were systematically performed. Co-registration was performed utilizing the carotid bifurcation as an anatomical landmark. Briefly, the out of plane resolution (slice thickness) was 1 mm, which allowed us to measure the position from the bifurcation and match the histology with the MRI. In order to avoid post-mortem thrombus formation, Heparin (100 IU/kg) was injected 10 min before euthanasia. Animals were sacrificed via an overdose of isoflurane. Transcardiac

perfusions through the left ventricle were carried out with saline and paraformaldehyde (4%). Carotid arteries were excised, collected in OCT and frozen for histology. Counter-stained with combined Masson's Elastin technique and Hematoxylin and Eosin (H&E).

Results

In vitro binding of P975 and P977

The r_1 value of P975 was measured on a relaxometer (Minispec, etc. Bruker) and was shown to be 9 $s^{-1}mM^{-1}$ at 40 °C and 60 MHz. The specificity of P975, P977 and Tirofiban to $\alpha_{IIb}\beta_3$ integrin was evaluated by inhibition measurements of FITC-Fg binding to TRAP-stimulated platelets. We observed a concentration-dependent inhibition of FITC-Fg binding in presence of P975, P977 or Tirofiban (Figure 1). This inhibition was complete at higher concentrations and the calculated IC_{50} values were 2.1 ± 0.3 μM, 1.6 ± 0.2 μM and 20.4 ± 0.3 nM, for P975, P977 and Tirofiban, respectively. The Ki values for P975, P977 and Tirofiban calculated according to the Cheng-Prusoff equation were 1.5 μM, 1.1 μM and 14.3 nM, respectively. Gd-DOTA, used as reference, displayed no affinity for $\alpha_{IIb}\beta_3$ (data not shown).

Imaging of thrombus formation with intravital fluorescence macroscopy

In order to study the thrombus formation and emphasize the critical role of platelets in the AA model of thrombosis, intravital fluorescence macroscopy was used after injection of fluorescently labeled platelets and AA thrombus induction. As shown in Figure 2 and the video (supplemental data), activated platelets immediately started adhering to the vessel wall following AA application onto the carotid. The conversion of AA by cyclooxygenases (COXs) and particularly COX-2 into prostaglandin H2 (PGH2) is known to yield Thromboxane A2 (TxA2) and Prostaglandin E2 (PEG2) that induce platelet activation and thrombosis [21]. Accordingly, we observed small thrombi on the luminal side of the vessel wall, clustering and eventually forming a surface occluding thrombus. As the pulsatile blood flow inside the carotid was maintained, the formed thrombi eventually detached from the arterial wall and embolized in the circulation. However, the process of thrombosis kept forming as long as the AA surrounding the carotid was still present in sufficient concentrations. Presence of intra-arterial thrombosis was subsequently confirmed by histology (Figure 2C). In addition of demonstrating the critical role of platelets in AA induced thrombosis, these observations emphasized the necessity to more or less retain thrombi for the subsequent *in vivo* MR imaging. To that end, a loose but permanent ligation was applied on the carotid prior to thrombus induction.

In vivo MR imaging of activated platelets in the thrombosis model

Six microliters of AA at 200 mg/ml (or EtOH sham surgery) were applied periadventially for 1 minute to induce intra-arterial thrombosis in the right mouse carotid. Mice were placed in the MRI scanner and baseline scans were performed to obtain images prior to contrast agent injection. Subsequently, P975 or Gd-DOTA was injected via a catheter placed in the tail vein. Consecutive MRI scans were acquired every 14 minutes up to 2 hours post-injection and signal enhancement was calculated in both the thrombosed carotid and the contralateral carotid (negative control). In both groups, MRI allowed clear identification of both carotids at baseline by black blood imaging (Figure 3). The presence of a thrombus was already visible in the right carotid artery. Thirty minutes after contrast agent injection, an initial signal enhancement in the lumen of the thrombosed carotid artery and in the perivascular area was observed in both groups (Figure 3). This initial luminal enhancement was attributed to contrast agent molecules trapped in the mesh of the thrombus. However, the initial signal increase obtained with P975 was visibly more pronounced compared to Gd-DOTA. More importantly, in the animals injected with P975, the signal enhancement persisted over time and was still present 120 minutes after injection (Figure 3). On the other hand, the animals injected with Gd-DOTA exhibited a rapid wash out of the contrast agent from the lesion after 30 min. This was confirmed

by MRI data quantification (Figure 5). Indeed, the ΔCNR values obtained in the injured carotid with P975 injection were significantly increased at each imaging time point compared to the values obtained with Gd-DOTA injection as well as the control and sham carotids (Figure 5). This was especially visible 2 hours post-injection when the ΔCNR values in the injured carotid of animals injected with P975 showed a 4-fold increase compared to the Gd-DOTA group, a 7-fold increase compared to the sham surgery group and a 8-fold increase compared to the control group ($P<0.01$). Therefore, P975 allowed accurate and efficient imaging of thrombosis.

In vivo study of P975 specificity to activated platelets

To evaluate the specificity of P975 to activated platelet-rich thrombi *in vivo*, we performed a competitive inhibition experiment. Eptifibatide, a clinical antagonist for $\alpha_{IIb}\beta_3$ receptors, was injected at a saturating dose prior to P975 injection. MRI scans were performed to obtain pre-contrast images, Eptifibatide and P975 were injected and the post-contrast MRI routine was applied. The injection of Eptifibatide did not induce thrombolysis. An initial signal increase in the thrombosed carotid artery was observed 30 minutes after contrast agent injection. However the signal increase did not persist throughout the 120 minutes window of imaging time and the washout kinetics of P975 in this cohort was very similar to that of the non-specific contrast agent Gd-DOTA (Figure 4). The absence of sustained contrast enhancement is likely due to the saturation of activated $\alpha_{IIb}\beta_3$ integrins on activated platelets by Eptifibatide. The data quantification at 120 minutes after injection in this cohort corroborated the observations as the increase in ΔCNR values were comparable to the ones obtained in the control animals injected with Gd-DOTA (Figure 5).

Discussion

In the present study, we demonstrated the *in vitro* affinity of a novel contrast agent (P975) to the activated integrin $\alpha_{IIb}\beta_3$ specifically expressed on activated platelets. We then showed its *in vivo* specificity in an AA model of thrombosis induced in the mouse carotid artery.

Real time observation of thrombi formation and embolization with intravital fluorescence microscopy demonstrated the critical role of activated platelets in the process of AA-induced thrombosis. The observation of embolization showed the necessity to keep the thrombi collected in order to obtain sufficient temporal resolution to perform MRI for thrombus detection pre and post-contrast. To address this, the diameter of the vessel was slightly reduced up-stream with a loosely applied permanent ligation. This ensured that even in case of emboli, the thrombi formed would be retained at the site of imaging. To ensure that the ligation did not induce thrombi formation, a sham surgery group where animals only underwent slight carotid ligation and received EtOH instead of AA showed an absence of intra-arterial thrombosis. This confirmed that the ligation did not affect thrombosis.

P975 is a contrast agent directed against the activated platelet fibrinogen receptor $\alpha_{IIb}\beta_3$. $\alpha_{IIb}\beta_3$ is an important therapeutic target in acute coronary syndromes due to its central role in the pathway of platelet activation [3]. The abundance of $\alpha_{IIb}\beta_3$ as well as its specific change of conformation on activated platelets makes it an ideal target for imaging. The binding of adhesive proteins to the $\alpha_{IIb}\beta_3$ integrin has been shown to occur through the peptide sequence Arg-Gly-Asp (RGD) amongst some others 26. The RGD sequence is found on fibrinogen, fibronectin, von Willebrand factor, vitronectin, thrombospondin and type I collagen 27–30. The contrast agent P975 used in this study is composed of a cyclic RGD peptide (P977) attached to a single Gd-moiety. *In vitro* experiments demonstrated the affinity of P975 and its peptide P977 for the $\alpha_{IIb}\beta_3$ integrin expressed on human activated platelets with an IC_{50} value in the micromolar range. In order to ensure sufficient detection of this mono-Gd chelate and specific thrombus enhancement with such moderate affinity, a high dose of P975 was tested. The initial dose of 100 μmol Gd/kg showed a 3.5 fold increase of the ΔCNR of the thrombus compared

to Gd-DOTA (non-specific contrast agent) at 120 minutes post-injection. However, given the relatively low molecular weight of P975 (1344 Da), we expect the contrast agent to have the ability to diffuse inside the clot thereby increasing the relative volume of enhancement in a given voxel. Therefore further investigations will be required to establish an optimal dose.

MRI protocols allowed facile localization of both carotid arteries pre and post-contrast images in corresponding slices. High spatial-resolution MR imaging reducing the partial volume effect and giving high signal to noise ratios (SNR) were applied since it was previously shown that clot detection decreased rapidly with decreasing spatial resolution [31]. The contrast effect provided by P975 persisted throughout time in the lumen of the injured carotid whereas the signal emanating from circulating unbound contrast agent was progressively cleared from the circulation. In some cases, P975 was also shown to accumulate in the region of both of the salivary glands at 2 hours post-injection. Likely, this indicated the presence of activated platelets due to the invasive surgery undergone for thrombus induction. Thus, P975 allowed accurate and specific detection of activated platelets and thrombi location, regardless of their size. Conversely, as expected the non-specific Gd-DOTA did not display any persistent signal enhancement and did not specifically enhance the thrombi.

In the literature, the P975 composing peptide was also reported to bind to $\alpha_V\beta_3$ integrins expressed by tumor cells with a dissociation constant (Kd) of 17 μM [22]. Therefore, it is likely that P975 may bind with approximately the same affinity to both types of integrins $\alpha_V\beta_3$ and $\alpha_{IIb}\beta_3$. However, it has been reported that there is a 40-fold greater number of $\alpha_{IIb}\beta_3$ integrins compared to $\alpha_V\beta_3$ epitopes expressed on activated platelets [32]. Therefore we can assume that P975 will primarily allow the detection of $\alpha_{IIb}\beta_3$ integrins in the AA-induced mouse model of carotid thrombosis. In order to validate this hypothesis and prove further specificity of P975 to the $\alpha_{IIb}\beta_3$ integrin, we decided to perform a competitive inhibition experiment with P975 using Eptifibatide, a $\alpha_{IIb}\beta_3$ blocker routinely used in patients hospitalized with unstable angina. Eptifibatide is a cyclic heptapeptide derived from RGD by the substitution of the single amino acid lysine for arginine [33]. It is described as a non-immunogenic, potent and rapidly reversible inhibitor of $\alpha_{IIb}\beta_3$ that is highly specific for $\alpha_{IIb}\beta_3$ and showed little affinity to other integrins. It was shown to block the binding of the ligands fibrinogen and von Willebrand factor without affecting the binding properties of other integrins therefore demonstrating its high affinity to the $\alpha_{IIb}\beta_3$ receptor. Eptifibatide is routinely used in clinic to achieve platelet inhibition in acute coronary syndromes and monitoring the effect of such a therapeutic intervention would be valuable for the management of thrombotic diseases. We showed in this experiment that the use of Eptifibatide at a saturating dose prior to P975 injection suppressed the sustained signal of P975 in the lumen of the thrombosed carotid at 2 hours after injection. P975 only induced an initial enhancement of the thrombus 30 minutes post-injection before rapidly clearing out of the circulation. Contrary to what has been demonstrated *ex vivo* [34], injection of Eptifibatide did not dissolve thrombi *in vivo* as the carotid still appeared occluded on the MRI performed post-injection. This different behavior is likely to be explained by the formation of fibrin during the *in vivo* clotting process. Indeed, fibrin plays a crucial role in stabilizing thrombi and might prevent thrombi from dissolving in presence of anti-$\alpha_{IIb}\beta_3$ without the conjugate use of anticoagulant or thrombolytic therapy. In addition, the use of a ligation likely reduced the flow in the carotid and may have limited the potential for embolization in the first place. In this cohort, P975 displayed the behavior of an unbound circulating contrast agent that is almost identical to the non-specific contrast agent, Gd-DOTA. This phenomenon can be attributed to the profusion of anti-$\alpha_{IIb}\beta_3$ agent binding the activated $\alpha_{IIb}\beta_3$ receptors therefore prohibiting its ligation by P975 molecules. This experiment was particularly critical as $\alpha_v\beta_3$ can be expressed by smooth muscle cells (SMC) following vascular injury and may have resulted in a competing binding source of P975. In addition, it would be of interest for future experiments to study the effect of physiological doses of aspirin or thienopyridine on P975 enhanced imaging as they have both demonstrated to achieve platelet inhibition [35]

Other strategies to image thrombi via MRI were considered and published over the past years. In particular, the high amount of fibrin formation during the clotting process resulted in a target of choice for the molecular imaging of thrombosis. Consequently, the MR compound EP-2104R showed promising clinical applications [13–14–36–38]. It has been published that 50% of acute STEMI patients bore coronary thrombi for days or weeks before the event [39]. Therefore, the detection of thrombi via MRI may be a valuable diagnostic approach for the early detection and prevention of cardiovascular events in the most at-risk patients. Further investigations are still however required before translating the presented technology to the clinic. The atherosclerotic plaque is characterized by chronic inflammation, which produces PGE2, amongst other mediators. Using the AA-induced model of thrombosis offers the advantage of exploring a model in which inflammation is predominant and is thus closer to atherothrombosis than other models. For example, the ferric chloride-induced model is characterized by very large areas of endothelium necrosis that are usually not seen in human pathological studies. However, the AA model of thrombosis does not necessarily account for the complex process of thrombosis upon spontaneous plaque rupture. Moreover, the expression of vitronectin may result in a source of non-specific background signal as we expect P975, an RGD analog, to bind to $\alpha_v\beta_3$-integrin. Nevertheless, SMC in the intima of potentially vulnerable plaques comprise only a small fraction as compared to the formed thrombi. Overall, the exploration of P975 in a model atherothrombosis is of a high-interest in order to determine the clinical relevance of the probe P975. In addition, the translation from high-field imaging to clinical imager would result in a loss of spatial resolution and signal to noise ratio (SNR), although the relaxivity of P975 is significantly higher at these lower field strengths. It is to be investigated how these changes would affect the detection of P975 as well as the identification of microthrombi that may precede ACS/STEMI. Indeed, this study demonstrated the enhancement of nearly occlusive thrombi and given the much lower spatial resolution of clinical MRI systems, it is unclear whether P975-enahnced MRI would allow the clinical detection of platelet-rich microthrombi in small vessels like the coronary. Another limitation of this study is that many of these microthrombi are likely to be of subacute age. It has previously been shown that platelet-targeted imaging of subacute thrombi yielded lower signal intensities when compared to acute thrombi [40]. This might therefore impair the detection of subacute thrombi via an activated platelet-targeted approach such as P975-enhanced MRI. We will focus future studies on imaging variously aged thrombi in a variety of animal models to further investigate the overall potential of P975.

Conclusions

The detection of activated platelets via non-invasive molecular MRI could not only become an important tool for the clinic but could also provide information on the pathophysiology of thrombosis, embolism and atherothrombosis. We were able to image AA-induced thrombosis using a contrast agent that specifically binds to the activated $\alpha_{IIb}\beta_3$ expressed on activated platelets. P975 displayed excellent contrast properties as well as high resolution and sensitive *in vivo* imaging of platelet-rich acute thrombi. Thus, P975 represents a novel non-invasive imaging tool for thrombi detection. However, further investigations are still required to demonstrate the overall clinical implications of this study.

Supplementary Material

Refer to Web version on PubMed Central for supplementary material.

References

1. Sanz J, Fayad ZA. Imaging of atherosclerotic cardiovascular disease. Nature 2008;451:953–957. [PubMed: 18288186]

2. Fuster V, Moreno PR, Fayad ZA, Corti R, Badimon JJ. Atherothrombosis and high-risk plaque: part I: evolving concepts. J Am Coll Cardiol 2005;46:937–954. [PubMed: 16168274]
3. Gawaz M, Langer H, May AE. Platelets in inflammation and atherogenesis. J Clin Invest 2005;115:3378–3384. [PubMed: 16322783]
4. Massberg S, Brand K, Grüner S, Page S, Müller E, Müller I, Bergmeier W, Richter T, Lorenz M, Konrad I, Nieswandt B, Gawaz M. A critical role of platelet adhesion in the initiation of atherosclerotic lesion formation. J Exp Med 2002;196:887–896. [PubMed: 12370251]
5. Anderson JL, Adams CD, Antman EM, Bridges CR, Califf RM, Casey DE, Chavey WE, Fesmire FM, Hochman JS, Levin TN, Lincoff AM, Peterson ED, Theroux P, Wenger NK, Wright RS, Smith SC, Jacobs AK, Halperin JL, Hunt SA, Krumholz HM, Kushner FG, Lytle BW, Nishimura R, Ornato JP, Page RL, Riegel B. American College of Cardiology, American Heart Association Task Force on Practice Guidelines (Writing Committee to Revise the 2002 Guidelines for the Management of Patients With Unstable Angina/Non-ST-Elevation Myocardial Infarction), American College of Emergency Physicians, Society for Cardiovascular Angiography and Interventions, Society of Thoracic Surgeons, American Association of Cardiovascular and Pulmonary Rehabilitation Society for Academic Emergency Medicine. ACC/AHA 2007 guidelines for the management of patients with unstable angina/non-ST-Elevation myocardial infarction: a report of the American College of Cardiology/American Heart Association Task Force on Practice Guidelines (Writing Committee to Revise the 2002 Guidelines for the Management of Patients With Unstable Angina/Non-ST-Elevation Myocardial Infarction) developed in collaboration with the American College of Emergency Physicians, the Society for Cardiovascular Angiography and Interventions, and the Society of Thoracic Surgeons endorsed by the American Association of Cardiovascular and Pulmonary Rehabilitation and the Society for Academic Emergency Medicine. J Am Coll Cardiol 2007;50:e1–e157. [PubMed: 17692738]
6. Briley-Saebo KC, Mulder WJ, Mani V, Hyafil F, Amirbekian V, Aguinaldo JG, Fisher EA, Fayad ZA. Magnetic resonance imaging of vulnerable atherosclerotic plaques: current imaging strategies and molecular imaging probes. J Magn Reson Imaging 2007;26:460–479. [PubMed: 17729343]
7. Choudhury RP, Fuster V, Fayad ZA. Molecular, cellular and functional imaging of atherothrombosis. Nat Rev Drug Discov 2004;3:913–925. [PubMed: 15520814]
8. Chu B, Phan BA, Balu N, Yuan C, Brown BG, Zhao XQ. Reproducibility of carotid atherosclerotic lesion type characterization using high resolution multicontrast weighted cardiovascular magnetic resonance. J Cardiovasc Magn Reson 2006;8:793–799. [PubMed: 17060101]
9. Jaffer FA, Libby P, Weissleder R. Molecular imaging of cardiovascular disease. Circulation 2007;116:1052–1061. [PubMed: 17724271]
10. Larose E, Kinlay S, Selwyn AP, Yeghiazarians Y, Yucel EK, Kacher DF, Libby P, Ganz P. Improved characterization of atherosclerotic plaques by gadolinium contrast during intravascular magnetic resonance imaging of human arteries. Atherosclerosis 2008;196:919–925. [PubMed: 17391676]
11. Sosnovik DE, Nahrendorf M, Weissleder R. Molecular magnetic resonance imaging in cardiovascular medicine. Circulation 2007;115:2076–2086. [PubMed: 17438163]
12. Helft G, Worthley SG, Fuster V, Fayad ZA, Zaman AG, Corti R, Fallon JT, Badimon JJ. Progression and regression of atherosclerotic lesions: monitoring with serial noninvasive magnetic resonance imaging. Circulation 2002;105:993–998. [PubMed: 11864931]
13. Sirol M, Aguinaldo JG, Graham PB, Weisskoff R, Lauffer R, Mizsei G, Chereshnev I, Fallon JT, Reis E, Fuster V, Toussaint JF, Fayad ZA. Fibrin-targeted contrast agent for improvement of in vivo acute thrombus detection with magnetic resonance imaging. Atherosclerosis 2005;182:79–85. [PubMed: 16115477]
14. Sirol M, Fuster V, Badimon JJ, Fallon JT, Moreno PR, Toussaint JF, Fayad ZA. Chronic thrombus detection with in vivo magnetic resonance imaging and a fibrin-targeted contrast agent. Circulation 2005;112:1594–1600. [PubMed: 16145001]
15. von zur Muhlen C, von Elverfeldt D, Moeller JA, Choudhury RP, Paul D, Hagemeyer CE, Olschewski M, Becker A, Neudorfer I, Bassler N, Schwarz M, Bode C, Peter K. Magnetic resonance imaging contrast agent targeted toward activated platelets allows in vivo detection of thrombosis and monitoring of thrombolysis. Circulation 2008;118:258–267. [PubMed: 18574047]

16. Zhao C, Shuke N, Okizaki A, Yamamoto W, Sato J, Iwata K, Kanno T, Hasebe N, Kikuchi K, Aburano T. Naturally formed coronary arterial thrombus detected by In-111 oxine platelet imaging. Clin Nucl Med 2005;30:492–495. [PubMed: 15965327]
17. Bates SM, Lister-James J, Julian JA, Taillefer R, Moyer BR, Ginsberg JS. Imaging characteristics of a novel technetium Tc 99m-labeled platelet glycoprotein IIb/IIIa receptor antagonist in patients With acute deep vein thrombosis or a history of deep vein thrombosis. Arch Intern Med 2003;163:452–456. [PubMed: 12588204]
18. Dunzinger A, Hafner F, Schaffler G, Piswanger-Soelkner JC, Brodmann M, Lipp RW. 99mTc-apcitide scintigraphy in patients with clinically suspected deep venous thrombosis and pulmonary embolism. Eur J Nucl Med Mol Imaging 2008;35:2082–2087. [PubMed: 18618107]
19. Taillefer R. Radiolabeled peptides in the detection of deep venous thrombosis. Semin Nucl Med 2001;31:102–123. [PubMed: 11330782]
20. Wang X, Xu L. An optimized murine model of ferric chloride-induced arterial thrombosis for thrombosis research. Thromb Res 2005;115:95–100. [PubMed: 15567459]
21. Gross S, Tilly P, Hentsch D, Vonesch JL, Fabre JE. Vascular wall-produced prostaglandin E2 exacerbates arterial thrombosis and atherothrombosis through platelet EP3 receptors. J Exp Med 2007;204:311–320. [PubMed: 17242161]
22. Montet X, Montet-Abou K, Reynolds F, Weissleder R, Josephson L. Nanoparticle imaging of integrins on tumor cells. Neoplasia 2006;8:214–222. [PubMed: 16611415]
23. Yamada T, Kidera A. Tailoring echistatin to possess higher affinity for integrin alpha(IIb)beta(3). FEBS Lett 1996;387:11–15. [PubMed: 8654558]
24. Xia Z, Wong T, Liu Q, Kasirer-Friede A, Brown E, Frojmovic MM. Optimally functional fluorescein isothiocyanate-labelled fibrinogen for quantitative studies of binding to activated platelets and platelet aggregation. Br J Haematol 1996;93:204–214. [PubMed: 8611461]
25. Schwarz M, Meade G, Stoll P, Ylanne J, Bassler N, Chen YC, Hagemeyer CE, Ahrens I, Moran N, Kenny D, Fitzgerald D, Bode C, Peter K. Conformation-specific blockade of the integrin GPIIb/IIIa: a novel antiplatelet strategy that selectively targets activated platelets. Circ Res 2006;99:25–33. [PubMed: 16778135]
26. Plow EF, Pierschbacher MD, Ruoslahti E, Marguerie GA, Ginsberg MH. The effect of Arg-Gly-Asp-containing peptides on fibrinogen and von Willebrand factor binding to platelets. Proc Natl Acad Sci U S A 1985;82:8057–8061. [PubMed: 3877935]
27. Hynes RO. Integrins: versatility, modulation, and signaling in cell adhesion. Cell 1992;69:11–25. [PubMed: 1555235]
28. Pierschbacher MD, Ruoslahti E. Cell attachment activity of fibronectin can be duplicated by small synthetic fragments of the molecule. Nature 1984;309:30–33. [PubMed: 6325925]
29. Plow EF, Pierschbacher MD, Ruoslahti E, Marguerie G, Ginsberg MH. Arginyl-glycyl-aspartic acid sequences and fibrinogen binding to platelets. Blood 1987;70:110–115. [PubMed: 3036276]
30. Ruoslahti E, Pierschbacher MD. New perspectives in cell adhesion: RGD and integrins. Science 1987;238:491–497. [PubMed: 2821619]
31. Johansson LO, Bjørnerud A, Ahlström HK, Ladd DL, Fujii DK. A targeted contrast agent for magnetic resonance imaging of thrombus: implications of spatial resolution. J Magn Reson Imaging 2001;13:615–618. [PubMed: 11276107]
32. Lawler J, Hynes RO. An integrin receptor on normal and thrombasthenic platelets that binds thrombospondin. Blood 1989;74:2022–2027. [PubMed: 2478219]
33. Scarborough RM, Naughton MA, Teng W, Rose JW, Phillips DR, Nannizzi L, Arfsten A, Campbell AM, Charo IF. Design of potent and specific integrin antagonists. Peptide antagonists with high specificity for glycoprotein IIb-IIIa. J Biol Chem 1993;268:1066–1073. [PubMed: 8419315]
34. Goto S, Tamura N, Ishida H. Ability of anti-glycoprotein IIb/IIIa agents to dissolve platelet thrombi formed on a collagen surface under blood flow conditions. J Am Coll Cardiol 2004;44:316–323. [PubMed: 15261925]
35. Raju NC, Eikelboom JW, Hirsh J. Platelet ADP-receptor antagonists for cardiovascular disease: past, present and future. Nat Clin Pract Cardiovasc Med 2008;5:766–780. [PubMed: 18957959]
36. Botnar RM, Buecker A, Wiethoff AJ, Parsons EC, Katoh M, Katsimaglis G, Weisskoff RM, Lauffer RB, Graham PB, Gunther RW, Manning WJ, Spuentrup E. In vivo magnetic resonance imaging of

coronary thrombosis using a fibrin-binding molecular magnetic resonance contrast agent. Circulation 2004;110:1463–1466. [PubMed: 15238457]

37. Spuentrup E, Katoh M, Buecker A, Fausten B, Wiethoff AJ, Wildberger JE, Haage P, Parsons EC, Botnar RM, Graham PB, Vettelschoss M, Günther RW. Molecular MR imaging of human thrombi in a swine model of pulmonary embolism using a fibrin-specific contrast agent. Invest Radiol 2007;42:586–595. [PubMed: 17620942]
38. Spuentrup E, Katoh M, Wiethoff AJ, Buecker A, Botnar RM, Parsons EC, Guenther RW. Molecular coronary MR imaging of human thrombi using EP-2104R, a fibrin-targeted contrast agent: experimental study in a swine model. Rofo 2007;179:1166–1173. [PubMed: 17948194]
39. Rittersma SZ, van der Wal AC, Koch KT, Piek JJ, Henriques JP, Mulder KJ, Ploegmakers JP, Meesterman M, de Winter RJ. Plaque instability frequently occurs days or weeks before occlusive coronary thrombosis: a pathological thrombectomy study in primary percutaneous coronary intervention. Circulation 2005;111:1160–1165. [PubMed: 15723983]
40. Knight LC, Primeau JL, Siegel BA, Welch MJ. Comparison of In-111-labeled platelets and iodinated fibrinogen for the detection of deep vein thrombosis. J Nucl Med 1978;19:891–894. [PubMed: 682021]

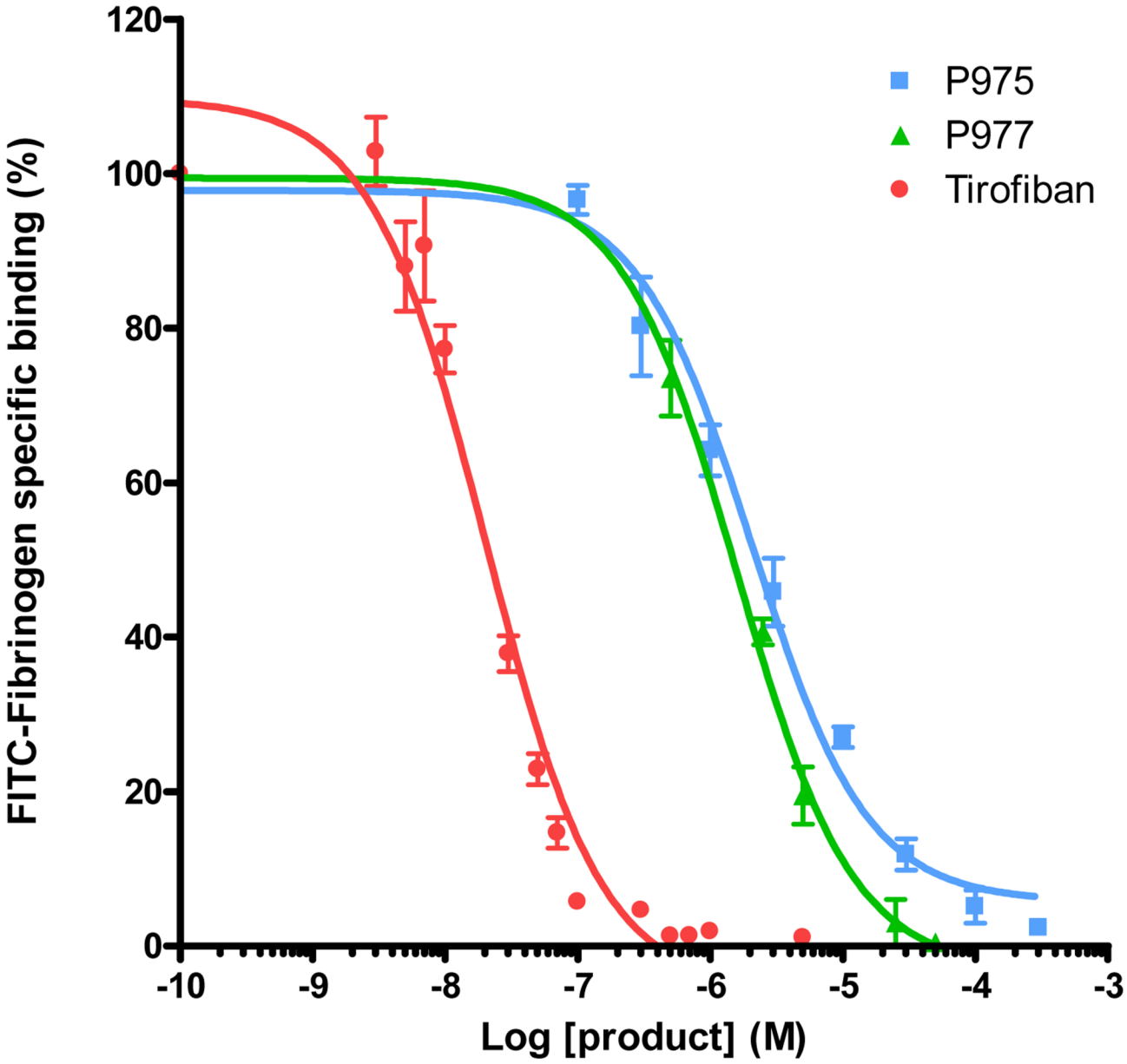

FIGURE 1.
Quantification of FITC-Fibrinogen specific binding to TRAP-simulated platelets as a function of increasing concentration of Tirofiban (positive control), P977 ($\alpha_{IIb}\beta_3$ targeted peptide) and P975 ($\alpha_{IIb}\beta_3$ targeted peptide attached to a Gd-DOTA moeity)

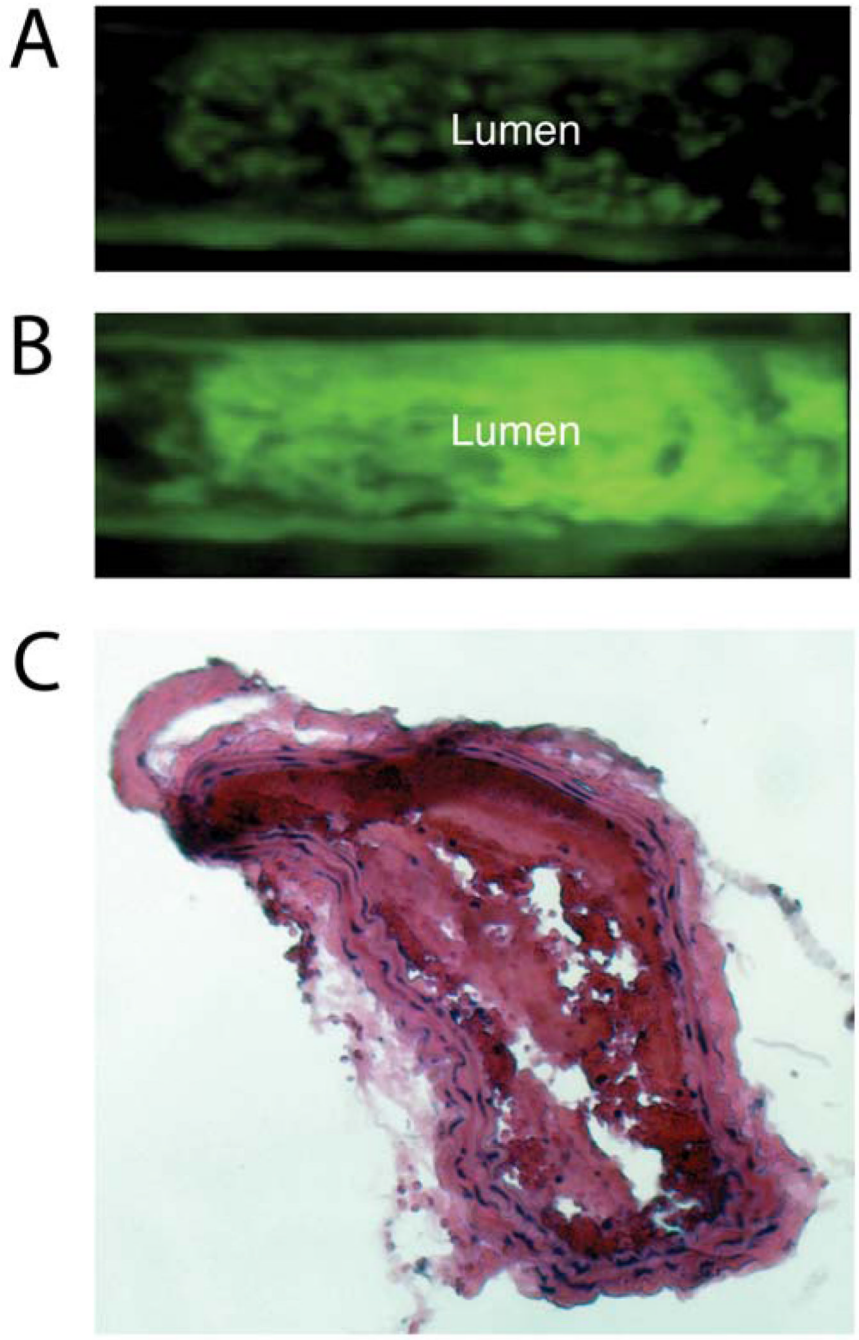

FIGURE 2.

A-B. Fluorescent intravital microscopy of an arachidonic acid (AA) induced model of thrombosis at two different time points. Platelets were isolated, labeled with an intracellular fluorophore (Calcein AM) and injected in a receiving mouse that underwent AA thrombosis. The vessel was placed under a fluorescent microscope and platelet aggregation was monitored. The platelets started adhering onto the vessel wall (A) and as the process of thrombosis continued, they aggregated towards the inside forming an intra-luminal thrombus (B). C. Histological section of the intra-arterial thrombus induced by periadventitial delivery of AA stained with H&E.

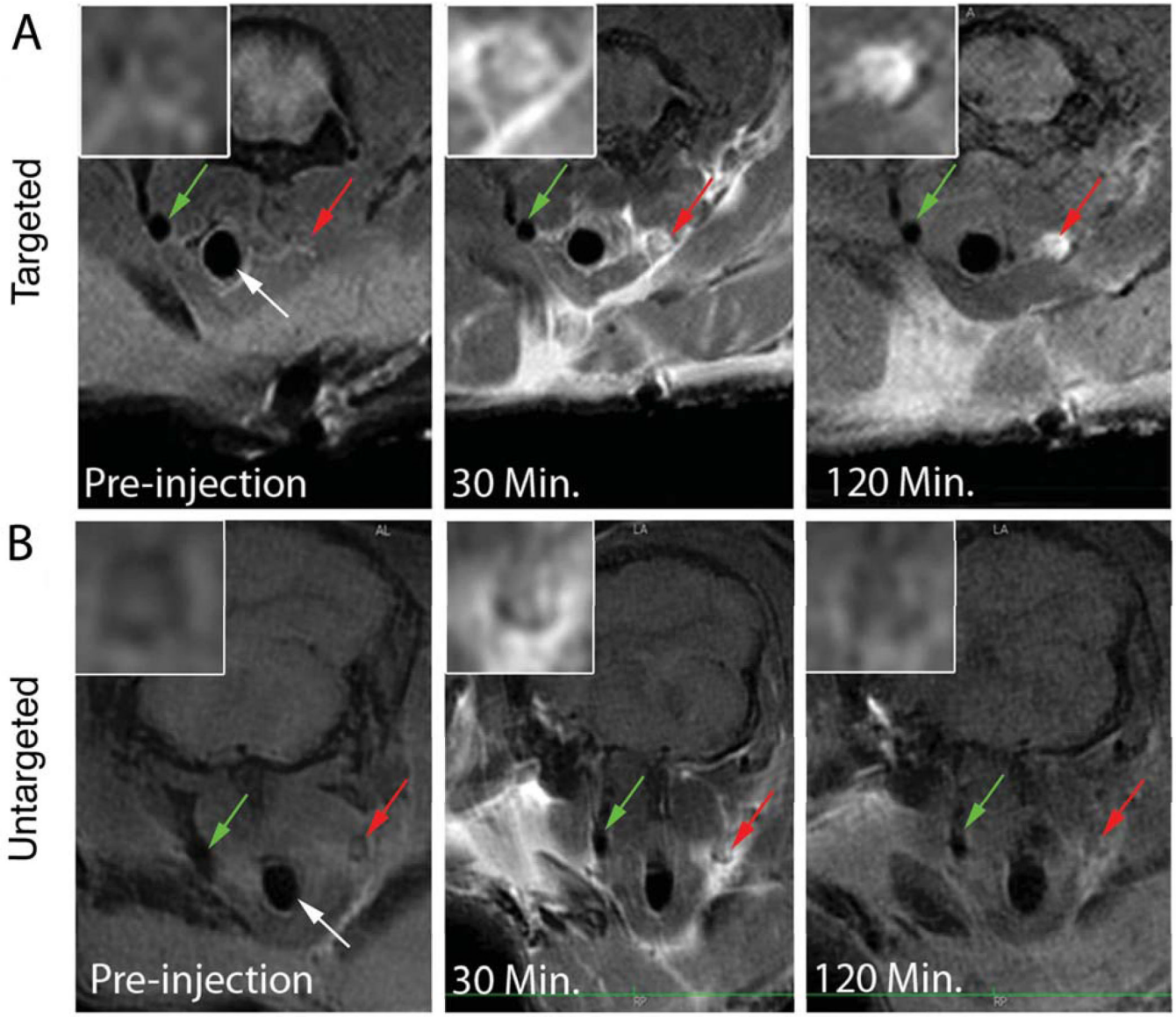

FIGURE 3.

In vivo MRI after AA-induced arterial thrombosis. The Trachea (white arrow), the non-injured left carotid (control, green arrow) and the injured right carotid (red arrow), are shown. Inserts in the upper left angle of each image represent magnification images of the injured carotid section. The panel A displays the behavior of P975 over 2 hours after its injection in thrombus-induced animals versus Gadolinium shown below in panel B. Before contrast agent injection, cross sections depict an occluded right carotid artery while the left carotid is visible on a T1-weighted black blood sequence. After injection of P975, signal intensity in the lumen of the thrombosed carotid increased at 30 minutes post-injection and persisted at 120 minutes. Conversely, Gd-DOTA only showed signal enhancement 30 minutes after injection and rapidly cleared from the circulation. Some non-specific perivascular enhancement was observed in both cases at early time points. No signal enhancement was observed in the contralateral carotid (negative control).

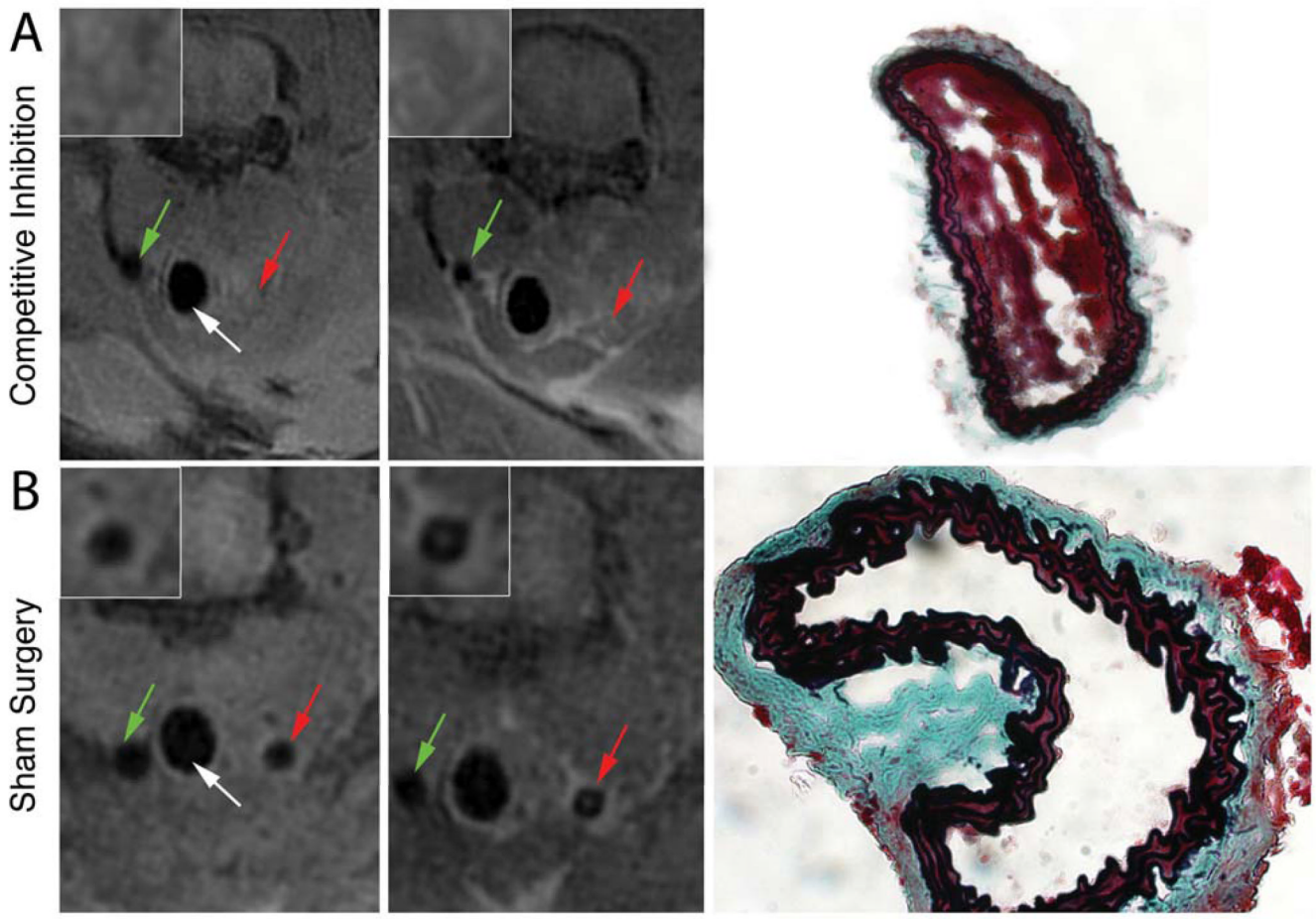

FIGURE 4.

MRI Cross sections of the non-injured (green arrow) and the injured (red arrow) carotid arteries. The trachea is shown (white arrows). Inserts in the upper left angle of each image represent magnification images of the injured carotid section. (A) Platelet inhibitor Eptifibatide was injected at a saturating dose after thrombus induction and before administration of P975. Although the presence of intra-luminal thrombosis was confirmed by histology using a modified Masson's Trichrome staining, the results showed no signal enhancement at 2 hours when compared to baseline in the injured carotid. (B) No MRI signal enhancement or thrombosis was visible in the injured carotid of animals who received the sham surgery *i.e.* delivery of EtOH and slight reduction of carotid diameter. Absence of intraluminal thrombosis was confirmed by histology in these animals.

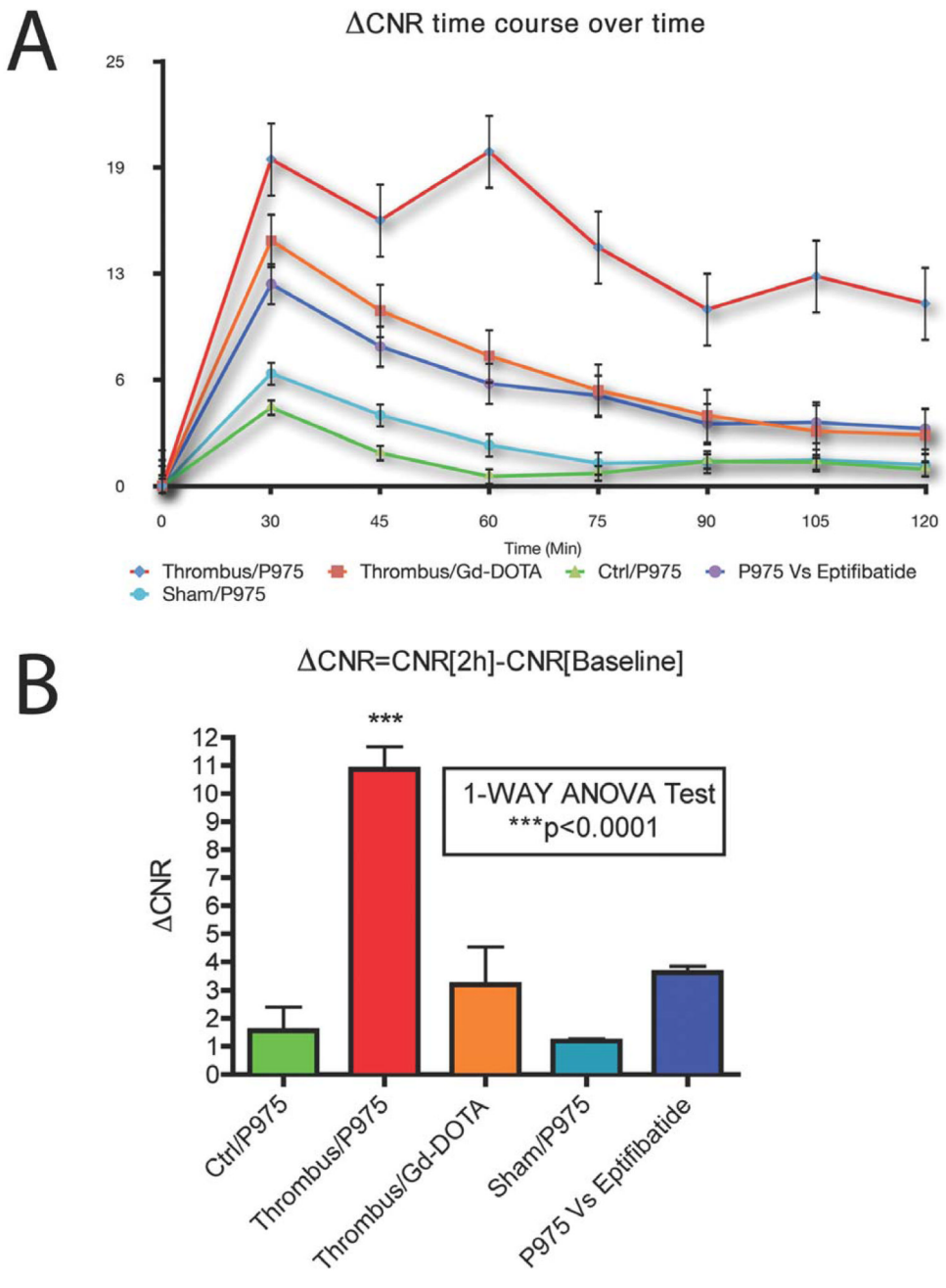

FIGURE 5.

Quantification of signal increases in the carotid artery lumens. (A) ΔCNRs were calculated at each imaging time point and plotted (0 represents the baseline scan). After Gd-DOTA injection, an initial signal increase occurred at 30 minutes post-injection (red line) possibly due to contrast agent molecules being transiently trapped within the mesh of the thrombus. Eventually, the values returned close to baseline over time. In contrast, P975 injection caused a signal increase that was still significantly higher compared to Gd-DOTA at 120 minutes post-injection (dark blue line). Animals injected with Eptifibatide prior to P975 (purple line) exhibited a similar behavior compared to animals injected with Gd-DOTA. The control groups (turquoise blue

and green lines) did not show any enhancement. (B) At 2 hours post injection P975 exhibited a significant increase in ΔCNRs compared to the rest of the groups.